Plant Physiology, January 1999, Vol. 119, pp. 277–287, www.plantphysiol.org © 1999 American Society of Plant Physiologists

A Steep Dependence of Inward-Rectifying Potassium Channels on Cytosolic Free Calcium Concentration Increase Evoked by Hyperpolarization in Guard Cells[1]

Alexander Grabov and Michael R. Blatt*

Laboratory of Plant Physiology and Biophysics, University of London, Wye College, Wye, Kent TN25 5AH, United Kingdom

Inactivation of inward-rectifying K^+ channels ($I_{K,in}$) by a rise in cytosolic free $[Ca^{2+}]$ ($[Ca^{2+}]_i$) is a key event leading to solute loss from guard cells and stomatal closure. However, $[Ca^{2+}]_i$ action on $I_{K,in}$ has never been quantified, nor are its origins well understood. We used membrane voltage to manipulate $[Ca^{2+}]_i$ (A. Grabov and M.R. Blatt [1998] Proc Natl Acad Sci USA 95: 4778–4783) while recording $I_{K,in}$ under a voltage clamp and $[Ca^{2+}]_i$ by Fura-2 fluorescence ratiophotometry. $I_{K,in}$ inactivation correlated positively with $[Ca^{2+}]_i$ and indicated a K_i of 329 ± 31 nM with cooperative binding of four Ca^{2+} ions per channel. $I_{K,in}$ was promoted by the Ca^{2+} channel antagonists Gd^{3+} and calcicludine, both of which suppressed the $[Ca^{2+}]_i$ rise, but the $[Ca^{2+}]_i$ rise was unaffected by the K^+ channel blocker Cs^+. We also found that ryanodine, an antagonist of intracellular Ca^{2+} channels that mediate Ca^{2+}-induced Ca^{2+} release, blocked the $[Ca^{2+}]_i$ rise, and Mn^{2+} quenching of Fura-2 fluorescence showed that membrane hyperpolarization triggered divalent release from intracellular stores. These and additional results point to a high signal gain in $[Ca^{2+}]_i$ control of $I_{K,in}$ and to roles for discrete Ca^{2+} flux pathways in feedback control of the K^+ channels by membrane voltage.

Ca^{2+} underlies many fundamental regulatory processes in plants, including adaptive responses to abiotic environmental stress (Knight et al., 1996; Russell et al., 1996; McAinsh et al., 1997) and programmed cell death evoked by pathogen attack (Low and Merida, 1996; Hammondkosack and Jones, 1997). Coordination of changes in $[Ca^{2+}]_i$ and its integration with downstream response elements are central in coupling stimulus input to cellular response in these processes.

In stomatal guard cells, the best characterized higher-plant cell model, major downstream targets of $[Ca^{2+}]_i$ and their roles in stomatal function have been identified. Increasing $[Ca^{2+}]_i$ is known to inactivate $I_{K,in}$ and to activate Cl^- channels, events that bias plasma membrane transport for net efflux of osmotically active solute and a loss of turgor, which drives stomatal closure (Blatt and Grabov, 1997). Furthermore, changes in $[Ca^{2+}]_i$ are associated with ABA, CO_2, and the growth hormone auxin (Blatt and Grabov, 1997; McAinsh et al., 1997). These $[Ca^{2+}]_i$ signals have been observed to oscillate (McAinsh et al., 1995; Webb et al., 1996), characteristics that may constitute "Ca^{2+} signatures" to encode specific downstream responses (Berridge, 1996). Yet, despite the evidence for $[Ca^{2+}]_i$ signaling in guard cells, surprisingly little detail is known about the link between $[Ca^{2+}]_i$ changes and ion channel activity at the plasma membrane or about the mechanisms mediating such $[Ca^{2+}]_i$ changes. To our knowledge, in no instance have the characteristics of ion channel regulation by Ca^{2+} been quantified directly in any higher-plant cell.

We recently described the coupling of membrane voltage to $[Ca^{2+}]_i$, demonstrating that hyperpolarization, whether under a voltage clamp or in the presence of low $[K^+]_o$, evoked $[Ca^{2+}]_i$ increases in guard cells, and that the voltage threshold for $[Ca^{2+}]_i$ rise was profoundly altered by ABA (Grabov and Blatt, 1998). Our observations indicated a link to Ca^{2+} influx across the plasma membrane and raised questions about the efficacy of $[Ca^{2+}]_i$ in inactivating $I_{K,in}$ and about the contributions of intracellular Ca^{2+} release to the $[Ca^{2+}]_i$ signal. We have used membrane voltage to experimentally manipulate $[Ca^{2+}]_i$ and report that $I_{K,in}$ is strongly dependent on $[Ca^{2+}]_i$, consistent with a cooperative binding of four Ca^{2+} ions to effect inactivation. Additional experiments indicate that voltage-evoked $[Ca^{2+}]_i$ increases depend both on Ca^{2+} influx and on release of Ca^{2+} from intracellular stores. These results underscore the role of $[Ca^{2+}]_i$ as a high-gain "switch" in the control of $I_{K,in}$, and implicate $[Ca^{2+}]_i$ in feedback control linking membrane voltage to the activity of the K^+ channels.

MATERIALS AND METHODS

Plant Material

Broad bean (*Vicia faba* L. cv Bunyan, Bunyard Exhibition) plants were grown and epidermal strips prepared as described previously (Blatt and Armstrong, 1993). All opera-

[1] This work was supported by grants from the Gatsby Charitable Foundation, the Royal Society, Human Frontiers Science Program (no. RG95/303 M), and the European Community Biotech (no. CT96-0062). A.G. was supported by the British Biotechnology and Biological Sciences Research Council (grant no. 32/C098-1).

* Corresponding author; e-mail mblatt@wye.ac.uk; fax 44–1233–813–140.

Abbreviations: $[Ca^{2+}]_i$, cytosolic free $[Ca^{2+}]$; CICR, Ca^{2+}-induced Ca^{2+} release; f_{340}, f_{360}, f_{390}, fluorescence excited by 340, 360, and 390 nm light, respectively; $I_{K,in}$, $I_{K,out}$, inward- and outward-rectifying K^+ channels, respectively.

tions were carried out on a Zeiss Axiovert microscope fitted with Nomarski differential interference contrast optics with strips bathed in rapidly flowing solutions (10 mL/min [approximately 20 chamber volumes/min]) at 20°C to 22°C. The standard medium was prepared with 5 mM Mes titrated to its pK_a (= 6.1) with $Ca(OH)_2$ (final $[Ca^{2+}]$ approximately 1 mM). KCl and other compounds were included as required. Buffers and salts were from Sigma. All agonists/antagonists were from Calbiochem. In some experiments, Mes buffer was titrated with KOH, and $CaCl_2$ or $MnCl_2$ were added separately as required.

Electrophysiology and Photometry

Electrical recordings and iontophoretic injections were achieved with three-barreled microelectrodes coated with paraffin to reduce electrode capacitance and, unless noted, microelectrode barrels were filled with 200 mM potassium acetate to minimize salt leakage and salt-loading artifacts associated with the Cl^- anion (Blatt and Armstrong, 1993). Connection to the amplifier headstage was via a 1 M KCl/Ag-AgCl half-cell, and a matching half-cell and 1 M KCl-agar bridge served as the reference (bath) electrode. Membrane currents were measured by voltage clamp under microprocessor control (μLAB/μLAN, WyeScience, Wye, UK) using three-pulse protocols (sampling frequency, 2 kHz) and bipolar staircase duty cycles (Blatt and Armstrong, 1993). Voltage and current were also sampled at low frequency (64 Hz) concurrently with measurements of $[Ca^{2+}]_i$.

$[Ca^{2+}]_i$ was determined by ratio fluorescence with a microphotometer (Cairn, Faversham, UK) using the dye Fura-2 (Molecular Probes, Eugene, OR) excited at 340, 360, and 390 nm (10-nm half-bandwidth filter, Schott, Yonkers, NY). Fluorescence was recorded through a slit diaphragm after filtering with a 480-nm long-pass filter (Schott) and excluded microelectrode fluorescence. Dye loading was by iontophoresis (Blatt and Armstrong, 1993) and was judged successful by visual checks for cytoplasmic dye distribution and by stabilization of the fluorescence ratio signal. Measurements were calibrated (Grabov and Blatt, 1997), and experiments were generally carried out within the first 20 to 30 min after Fura-2 loading to avoid difficulties associated with bleaching and decay of the fluorescence signals.

Numerical Analysis

Data analysis was carried out by nonlinear, least-squares fitting (Marquardt, 1963) and, where appropriate, results are reported as the means ± SE of (n) observations.

RESULTS

K^+ Channel Inactivation Is a Consequence of $[Ca^{2+}]_i$ Elevation

Although current through $I_{K,in}$ was previously reported not to inactivate with time, past studies were generally limited by voltage-clamp steps to periods of 2 to 4 s (Blatt and Grabov, 1997; Thiel and Wolf, 1997) or, over longer times, were carried out with $[Ca^{2+}]_i$ buffers present at the cytosolic face of the membrane after exchange with patch-pipette solutions (Schroeder, 1988). By contrast, concurrent measurements of $[Ca^{2+}]_i$ and K^+ channel current in vivo showed a pronounced inactivation of $I_{K,in}$ evident only after the first 2 to 4 s of 20-s voltage steps to −200 mV and suggested a close link to moderate increases in $[Ca^{2+}]_i$ (Grabov and Blatt, 1998).

To relate $I_{K,in}$ inactivation to the voltage threshold initiating a $[Ca^{2+}]_i$ rise, guard cells loaded with Fura-2 were driven through slow, 2-min voltage ramps from +20 to −200 mV. f_{340}, f_{360}, and f_{390} light, as well as the f_{340}/f_{390} ratio as a measure of $[Ca^{2+}]_i$, were recorded concurrently with a membrane current under voltage clamp. Figure 1 shows the voltage, current, and fluorescence ratios recorded from one guard cell, with the time course of the $[Ca^{2+}]_i$ rise in Figure 1B calculated from f_{340}/f_{390} and the individual fluorescence signals shown in Figure 1D. The $[Ca^{2+}]_i$ signal increased appreciably, but only once the voltage was driven more negative than at about −120 mV (Grabov and Blatt, 1998). Note that no change was seen in the f_{360} trace with the voltage clamp in contrast to f_{340} and f_{390}, indicating that the changes in fluorescence were a consequence of changes in $[Ca^{2+}]_i$ rather than an effect of voltage on dye leakage or redistribution. Under similar voltage-clamp conditions (n = 55 cells), membrane hyperpolarization to −200 mV was accompanied by increases in $[Ca^{2+}]_i$ from a mean resting value of 202 ± 23 nM to values often in excess of 1 μM (Fig. 2C; mean ± SE, 703 ± 98 nM), and depolarizations were followed by recovery of $[Ca^{2+}]_i$ to the initial resting values.

The voltage-clamp record in Figure 1 shows that the rise in $[Ca^{2+}]_i$ was accompanied by a decline in the amplitude of inward membrane current. The initial clamp step to +20 mV in Figure 1C showed a large, outward (positive) current corresponding to the activation of $I_{K,out}$ at this voltage. As the voltage was driven to values between approximately −50 and −130 mV (at which, with 10 mM K^+ outside, $I_{K,out}$ is inactive) the current declined to close to 0. At voltages negative of about −140 mV a large, inward current was observed, consistent with the activation of the Ca^{2+}-sensitive $I_{K,in}$ (Lemtiri-Chlieh and MacRobbie, 1994; Grabov and Blatt, 1997). However, this inward current decayed in magnitude in this and in the other recordings as the voltage approached −200 mV, coincident with the rise in $[Ca^{2+}]_i$.

To quantify the effect of prolonged membrane hyperpolarization on $I_{K,in}$, measurements were compiled from 52 independent experiments in which the membrane voltage was driven stepwise to −200 mV for 20 s or longer. Again, the characteristics of $I_{K,in}$ were related to $[Ca^{2+}]_i$ through concurrent recordings of Fura-2 fluorescence. Examples of clamp-current and $[Ca^{2+}]_i$ recordings from two guard cells are shown in Figure 2, A and B. The voltage step for the cell in Figure 2A led to a small increase only in $[Ca^{2+}]_i$ (bottom trace). In this case, and in cells showing a similar $[Ca^{2+}]_i$ response, the inward current exhibited prolonged activation, with an apparent half-time near 100 ms, typical of $I_{K,in}$. This current remained stable or increased slowly

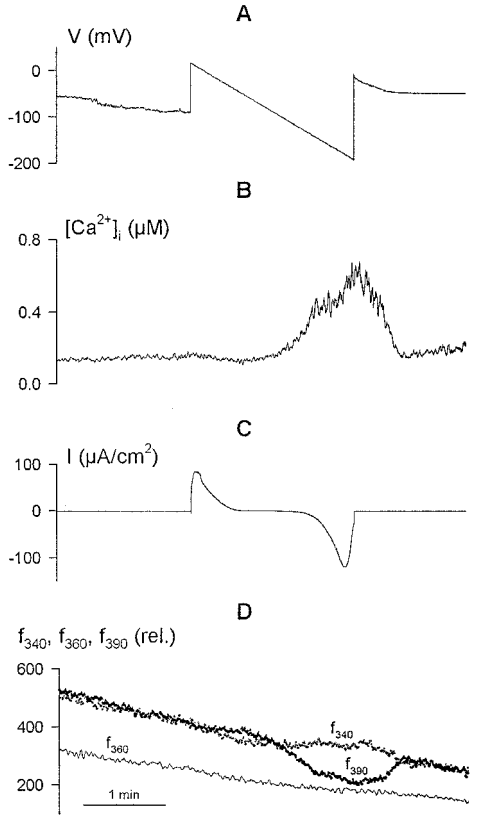

Figure 1. Voltage ramps demonstrate a voltage threshold for increases in $[Ca^{2+}]_i$ and consequent inactivation of current carried by $I_{K,in}$. Concurrent records of voltage (A), $[Ca^{2+}]_i$ (B), and clamp current (C) are shown, along with the raw Fura-2 fluorescence recorded on f_{340}, f_{360}, and f_{390} (D). Data are from one guard cell bathed in 5 mM Ca^{2+}-Mes, pH 6.1, with 10 mM KCl. Slowly ramping membrane voltage from +20 to −200 mV under voltage clamp was accompanied by an appreciable rise in $[Ca^{2+}]_i$ at voltages negative of about −120 mV. The outward (positive) current at the start of the voltage ramp is associated with $I_{K,out}$ (Blatt and Grabov, 1997). Activation of inward (negative) current at voltages negative of −120 mV, carried predominantly by $I_{K,in}$ (Blatt and Grabov, 1997), was followed by a near-complete decay in current amplitude during the final 10 s of the ramp and coincident with the $[Ca^{2+}]_i$ rise near and above 400 nM. Gradual decay in fluorescence recorded on excitation at all three wavelengths (D) is characteristic of progressive photobleaching of Fura-2 under these conditions. Note the absence any influence of the voltage ramp on the fluorescence trajectory recorded at the isobestic wavelength f_{360}.

thereafter during the 20-s period (Fig. 2A, top trace). In contrast, experiments in which hyperpolarization led to an appreciable increase in $[Ca^{2+}]_i$ (Fig. 2B, bottom trace) also showed a pronounced biphasic rise with a subsequent decline in the clamp-current amplitude after the first 2 to 4 s at −200 mV (Fig. 2B, top trace). A summary of all 52 experiments shows the positive correlation between the maximum change in $[Ca^{2+}]_i$ during clamp steps and the relative inactivation of the current measured at the end of the 20-s clamp step compared with that recorded 2 s after its start (Fig. 2C). We also noted a dependence of voltage-evoked $[Ca^{2+}]_i$ increases on the resting $[Ca^{2+}]_i$ level before stimulation (Fig. 2D). The analysis shows that the greatest rise in $[Ca^{2+}]_i$ was evoked from resting values around a median of 140 nM, whereas cells with resting $[Ca^{2+}]_i$ near and below 80 nM and above 300 nM generally showed less sensitivity to the voltage stimulus.

The causal relationship of $I_{K,in}$ inactivation to the $[Ca^{2+}]_i$ increases was confirmed in single guard cells using a standard two-pulse protocol with eight cycles of a 0.5-s conditioning step to −100 mV and 2-s steps to test voltages from +20 to −200 mV, by introducing additional 0.5-s voltage steps between cycles to manipulate $[Ca^{2+}]_i$. Figure 3 shows the results of two consecutive voltage-clamp protocols with the additional steps either to −250 mV (a) or to −30 mV (b). The current records are overlaid in Figure 3A in each case and show, in successive test pulses, the time-dependent outward current of $I_{K,out}$ evoked on positive voltage steps and $I_{K,in}$ on steps negative of −120 mV. Intervening steps to −250 mV yielded a cumulative rise in $[Ca^{2+}]_i$ (Fig. 3B, bottom trace) and gave rise to the final time-dependent inward current (a, numbered 1–8, corresponding to the numbered steps in Fig. 3B, top trace) that declined in magnitude with each cycle coincident with the rise in $[Ca^{2+}]_i$. However, intervening steps to −30 mV, which did not evoke a rise in $[Ca^{2+}]_i$, had little effect on $[Ca^{2+}]_i$ or on the K^+ current.

A cursory view of the last three cycles shows that $I_{K,in}$ evoked by the test voltage steps was greatly reduced in protocol a compared with the same steps in protocol b, coincident with the mean $[Ca^{2+}]_i$ elevation (solid bars over $[Ca^{2+}]_i$ trace) near 320 nM compared with 170 nM, respectively. In this case, analysis of the steady-state current showed a 73% reduction of $I_{K,in}$ after accounting for background (instantaneous) currents (Fig. 3C). Current at 0 mV, which is associated with $I_{K,out}$, was recorded before a significant rise in $[Ca^{2+}]_i$ and is known to be insensitive to $[Ca^{2+}]_i$ (Hosoi et al., 1988; Lemtiri-Chlieh and MacRobbie, 1994; Grabov and Blatt, 1997).

K^+ Channel Activity Shows a Steep Dependence on $[Ca^{2+}]_i$

To quantify the $[Ca^{2+}]_i$ sensitivity of $I_{K,in}$, a similar strategy of repeated hyperpolarizations was used to manipulate $[Ca^{2+}]_i$, and both current and Fura-2 fluorescence were measured concurrently. In this case, 20-s steps from a holding voltage of −50 to −200 mV were used to raise $[Ca^{2+}]_i$ and the intervals between steps decreased from 90 to 20 s to give an elevated background of $[Ca^{2+}]_i$ at the start of each subsequent step. $I_{K,in}$ was characterized after subtracting the background (instantaneous) current from measurements during the first 2 s of each step.

Figure 4A shows the results of measurements from one guard cell obtained at four different $[Ca^{2+}]_i$ values (in μM on right). The steady-state $I_{K,in}$ from these data are included in Figure 4B (solid symbols) along with the means ± SE of $I_{K,in}$ from another 52 guard cells binned over $[Ca^{2+}]_i$ intervals of 80 nM. The results demonstrate a steep dependence of $I_{K,in}$ on $[Ca^{2+}]_i$ that was most pronounced over the range from 200 to 500 nM $[Ca^{2+}]_i$. When subjected to nonlinear, least-squares fitting (Marquardt, 1963), the data could not be accommodated satisfactorily with a sim-

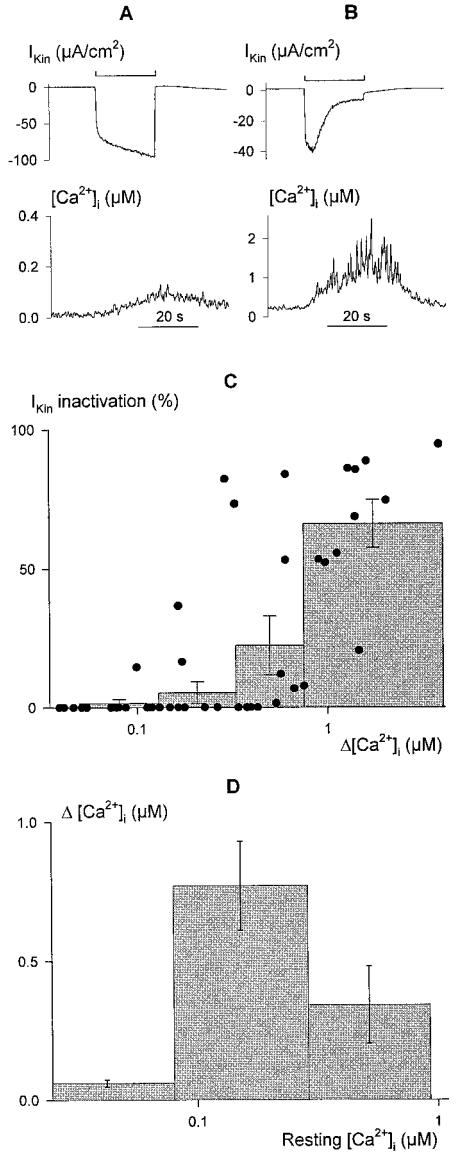

Figure 2. Inactivation of current through $I_{K,in}$ is correlated with $[Ca^{2+}]_i$ elevation. Voltage steps of 20 s duration from −50 to −200 mV leading to limited (A) and profound (B) increases in $[Ca^{2+}]_i$ (bottom trace, note different scales) in two broad bean guard cells. The clamp current (top trace, note different scales) shows the characteristic time course for $I_{K,in}$ activation (A) in the absence of an extensive rise in $[Ca^{2+}]_i$, and activation followed by a decay in current amplitude (B) with the more pronounced rise in $[Ca^{2+}]_i$. C, Summary of relative $I_{K,in}$ inactivation as a function of the change in $[Ca^{2+}]_i$ ($\Delta[Ca^{2+}]_i$) evoked by 20-s voltage steps from −50 to −200 mV recorded in 52 independent experiments (solid points). Histograms show the means ± SE of measurements binned in successive pools of 10 or 11 experiments. Inactivation of $I_{K,in}$ was calculated from the ratio $(I_{max} - I_{final})/I_{max}$, with I_{max} determined at maximum $I_{K,in}$ amplitude and I_{final} taken as the final current amplitude without correction for instantaneous current. $\Delta[Ca^{2+}]_i$ values were determined from the mean $[Ca^{2+}]_i$ recorded over periods of 1 s immediately before and at the end of the voltage steps. Note that the analysis does not account for measurements in which $[Ca^{2+}]_i$ was initially high, nor does it account for measurements in which clamp steps yielded little inward current. The distribution is therefore probably skewed to the right along the *x* axis, but nonetheless shows that current inactivation was associated with the rise in $[Ca^{2+}]_i$. D, $[Ca^{2+}]_i$ elevation ($\Delta[Ca^{2+}]_i$) after 20-s steps to −200 mV is dependent on the resting $[Ca^{2+}]_i$ level. Data from C plotted as a function of $[Ca^{2+}]_i$ before voltage steps to −200 mV. Histograms show the means ± SE of measurements binned in successive pools with $[Ca^{2+}]_i \leq 80$ nM, 80 nM $< [Ca^{2+}]_I \leq 300$ nM, and $[Ca^{2+}]_I > 300$ nM at rest. Note the logarithmic abscissa. The decline in the mean $\Delta[Ca^{2+}]_i$ from high starting $[Ca^{2+}]_i$ values is not consistent with saturation of the Fura-2 signal.

ple titration function of a single Ca^{2+}-binding site. Therefore, fittings were carried out using a formulation of the Hill equation (Hill, 1910):

$$I_K = \frac{I_{K,max} K_d^n}{K_d^n + [Ca^{2+}]_i^n}$$

where I_K and $I_{K,max}$ are the current and maximum current at −200 mV, respectively; K_d is the dissociation constant; and n is the cooperativity (Hill) coefficient and corresponds to the apparent number of Ca^{2+} ions binding per channel. Best fittings were obtained with a K_i of 329 ± 31 nM. Analyses carried out on a cell-by-cell basis (not shown) gave a similar K_i of 346 ± 22 nM. In every case, the analyses also yielded values for n close to 4 (mean ± SE, 4.1 ± 0.5 on a cell-by-cell basis), consistent with the cooperative action of at least four Ca^{2+} ions to inactivate $I_{K,in}$. Thus, the data indicate a profound sensitivity of the channels to relatively small changes in $[Ca^{2+}]_i$ above normal resting values, a point we will return to below.

Ca^{2+} Influx and the $[Ca^{2+}]_i$ Rise Are Independent of $I_{K,in}$

Previous experiments showed that the amplitude of voltage-evoked $[Ca^{2+}]_i$ increases were linearly related to the external Ca^{2+} concentration and were associated with Fura-2 quench when Mn^{2+} was substituted for external Ca^{2+} (Grabov and Blatt, 1998). These results and the dependence of $[Ca^{2+}]_i$ on negative membrane voltages suggested a specific Ca^{2+} influx triggered by the voltage across the plasma membrane. However, because $I_{K,in}$ also activates at these voltages, albeit over a much shorter time, it could be argued that the Ca^{2+} influx occurred through the K^+ channels. Ca^{2+} entry through the K^+ channels in guard cells has been proposed, based on tail-current-reversal analyses (Fairley-Grenot and Assmann, 1992).

To distinguish between these two possibilities, we recorded $[Ca^{2+}]_i$ and the channel current under voltage clamp during challenge with Ca^{2+} and K^+ channel antagonists. Figure 5A shows that adding 0.1 mM Gd^{3+}, a Ca^{2+} channel blocker (Klusener et al., 1995; Sedbrook et al., 1996), outside virtually eliminated the $[Ca^{2+}]_i$ transients evoked by subsequent voltage steps to −200 mV (bottom trace), while promoting the current associated with $I_{K,in}$ (top trace). Similar results were obtained from an additional four independent experiments with the Ca^{2+} channel blocker. Because Gd^{3+} may permeate the plant plasma membrane (Klusener et al., 1995), albeit slowly, we also explored the effects of higher-M_r peptide toxins that show specificity for plasma membrane Ca^{2+} channels in animals.

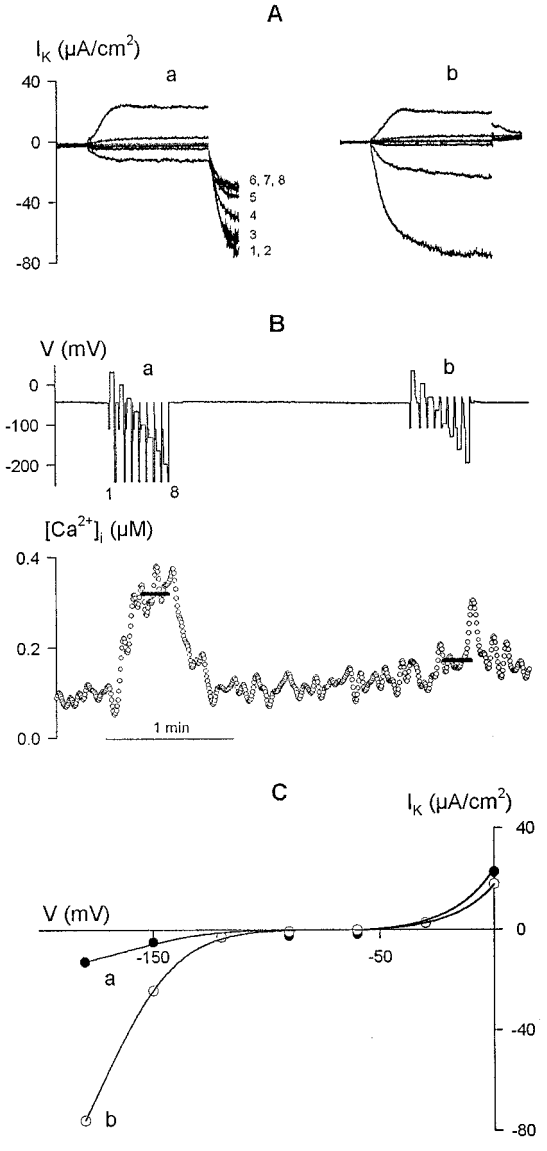

Figure 3. Inactivation of current through $I_{K,in}$ is evoked by $[Ca^{2+}]_i$ elevation. Data are from one guard cell bathed in 5 mM Ca^{2+}-Mes, pH 6.1, with 10 mM KCl. A, Clamp current recorded using standard two-pulse protocols of eight cycles with the addition of a third, 0.5-s intervening step at the end of each cycle to −250 mV (a) or to −30 mV (b). Clamp cycles: 0.5-s conditioning step, −100 mV; 2-s test steps (8) from +20 to −200 mV. B, Voltage (V, top trace) and $[Ca^{2+}]_i$ (bottom trace) records with intervening voltage steps numbered according to the cycle (1–8, cross-referenced to currents in A). The mean $[Ca^{2+}]_i$ during the final three cycles in each protocol is indicated by the solid lines overlaid on the $[Ca^{2+}]_i$ record. C, Steady-state current-voltage characteristic determined from the currents recorded at the end of the test voltage steps in protocols a and b. The curves have not been corrected for the background ("instantaneous") current.

Exposures to 0.5 μM calcicludine suppressed the $[Ca^{2+}]_i$ rise and relieved $I_{K,in}$ inactivation at −200 mV (Fig. 5B). Calcicludine is a 6.9-kD peptide toxin derived from *Dendroaspis augusticeps* venom and preferentially blocks L-type Ca^{2+} channels in animal tissues (Schweitz et al., 1994). The toxin is a highly charged, soluble protein and is therefore unlikely to pass across the plasma membrane. In contrast (not shown), the voltage-evoked $[Ca^{2+}]_i$ rise was unaffected by a peptide toxin, 1 μM ω-conotoxin (GVIIIa), and a specific N-type Ca^{2+} channel antagonist (Mori et al., 1991; Leveque et al., 1994). Substitution of external K^+ with Cs^+, which blocks the current through $I_{K,in}$ (Thiel and Wolf, 1997), had no measurable effect on the voltage-evoked $[Ca^{2+}]_i$ rise in each of the six experiments (not shown), and the $[Ca^{2+}]_i$ rise was insensitive to changes in external K^+ between 0.1 and 10 mM (Grabov and Blatt, 1998). These latter results, and the insensitivity of $I_{K,in}$ to Gd^{3+} and calcicludine compared with the $[Ca^{2+}]_i$ transients, implicate a unique class of Ca^{2+}-permeable channels at the plasma membrane that activate on hyperpolarization to

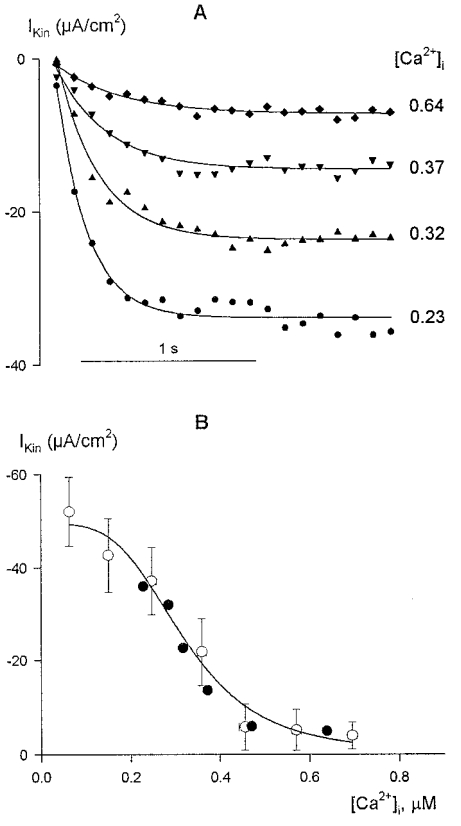

Figure 4. Inactivation of $I_{K,in}$ shows a steep dependence on $[Ca^{2+}]_i$ above resting $[Ca^{2+}]_i$ levels. A, Data are from one guard cell bathed in 5 mM Ca^{2+}-Mes, pH 6.1, with 10 mM KCl. $I_{K,in}$ recorded during the first 2 s of 20-s steps to −200 mV with $[Ca^{2+}]_i$ elevated by successively decreasing the interstep interval from 90 to 20 s. Data fitted to single-exponential activation curves and points are shown at 100-ms intervals for clarity. $[Ca^{2+}]_i$ is on the right (in μM). B, Summary of steady-state $I_{K,in}$ from A (solid symbols) along with means ± SE of data from 52 guard cells (open symbols) binned in pools of eight to nine experiments with increasing $[Ca^{2+}]_i$. $[Ca^{2+}]_i$ values were determined from the mean $[Ca^{2+}]_i$ recorded over the final 1 s of voltage steps after prior stimulation to raise $[Ca^{2+}]_i$ (see A) or from equivalent measurements from resting $[Ca^{2+}]_i$ conditions. The solid line is the result of nonlinear least-squares fitting of the means to the Hill equation (Eq. 1). Fitted parameters: K_i, 329 ± 31 nM; n (cooperativity coefficient), 4.1 ± 0.5. Statistically equivalent results were obtained when the data were fitted without binning (not shown).

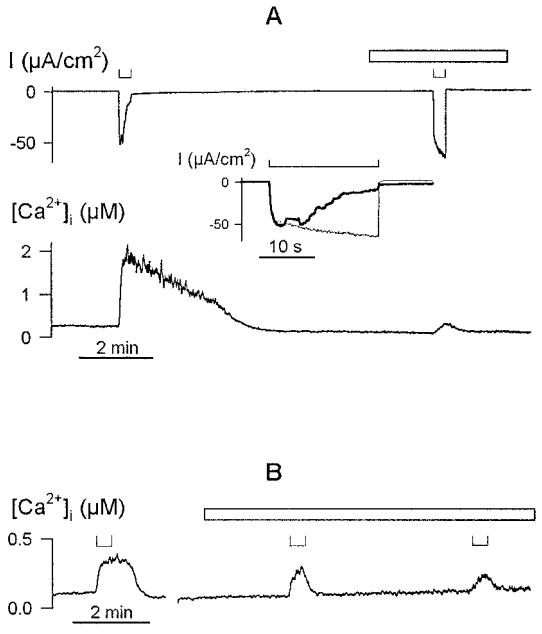

Figure 5. Voltage-evoked $[Ca^{2+}]_i$ rise is sensitive to extracellular Ca^{2+} channel blockers. A, $[Ca^{2+}]_i$ increases (trace below) and clamp current (trace above) during 20-s steps from −50 to −200 mV (⊔, above) before and after adding 0.1 mM $GdCl_3$ to the bath. Period of $GdCl_3$ exposure is indicated by the open bar. Data are from one guard cell in 5 mM Ca^{2+}-Mes, pH 6.1, with 10 mM KCl. Inset, Clamp current during steps to −200 mV (⊔, above) replotted on expanded time scale shows characteristic activation of the $I_{K,in}$ current (Grabov and Blatt, 1997) when the $[Ca^{2+}]_i$ rise is suppressed in the presence of Gd^{3+} (fine line) and its time-dependent inactivation when $[Ca^{2+}]_i$ rises in the absence of Gd^{3+} (solid line). B, $[Ca^{2+}]_i$ increases evoked during 20-s steps from −50 to −200 mV (⊔, above) before and after adding 0.5 μM calcicludine to the bath. Data are from one guard cell in 5 mM Ca^{2+}-Mes, pH 6.1, with 10 mM KCl. Period of exposure to the Ca^{2+} channel blocker is indicated by an open bar. Time scale (below), 2 min.

facilitate Ca^{2+} entry. The data also argue against a predominance of the Ca^{2+} flux through the K^+ channels (Fairley-Grenot and Assmann, 1992), a point we comment on in "Discussion."

Evoked $[Ca^{2+}]_i$ Increases Are Coupled to Cytosolic Ca^{2+} Release

Although the data above point to entry across the plasma membrane as the initial source of Ca^{2+} for the voltage-evoked $[Ca^{2+}]_i$ transients, intracellular Ca^{2+} stores have also been indicated in evoked $[Ca^{2+}]_i$ signals in guard cells (Blatt and Grabov, 1997; McAinsh et al., 1997; Grabov and Blatt, 1998). Analogous patterns of Ca^{2+} entry and subsequent release from intracellular stores are well known in animal cells and result from positive feedback of Ca^{2+} that activates intracellular Ca^{2+} release channels. Such CICR rapidly amplifies $[Ca^{2+}]_i$ signals and facilitates $[Ca^{2+}]_i$ spikes and oscillations (Clapham, 1995; Berridge, 1996).

To assess the contribution of intracellular Ca^{2+} release to the voltage-evoked $[Ca^{2+}]_i$ transients, we used a strategy of Fura-2 fluorescence quenching with Mn^{2+}, which passes through many Ca^{2+}-permeable channels (Fasolato et al., 1993; Pineros and Tester, 1995; Schofield and Mason, 1996; Striggow and Ehrlich, 1996). Its binding causes a loss of Fura-2 fluorescence that can be separated from the effects of $[Ca^{2+}]_i$ by recording the Fura-2 fluorescence emission at f_{360}, the isobestic wavelength. Thus, if the $[Ca^{2+}]_i$ rise depended on divalent release from intracellular stores, we reasoned that hyperpolarization should be followed by a stimulation of Fura-2 quenching once guard cells were loaded with Mn^{2+}.

For these experiments guard cells were exposed to 2 mM Mn^{2+} for 8 h to load intracellular Ca^{2+} stores with Mn^{2+} (Fasolato et al., 1993). Before the start of recordings, the guard cells were washed in Ca^{2+}-Mes buffer with 10 mM KCl to remove external Mn^{2+}. After impalements, membrane voltage was clamped to −50 mV and the cells were loaded with Fura-2 in the usual manner. Thereafter, Fura-2 fluorescence was recorded after excitation at 360 nm and the cells were challenged with membrane voltage steps to −200 mV. Results from one guard cell are shown in Figure 6A. Voltage steps to −200 mV resulted in a rise, and then a more rapid fall in f_{360} when Ca^{2+} was present outside. However, when Ca^{2+} was removed from the bath to prevent Ca^{2+} entry, triggering intracellular release, only a stepwise increase in f_{360} was seen and then only during the period that the voltage was clamped to −200 mV. In fact, comparing f_{360} quench immediately after the voltage steps showed that a 5.5-fold greater rate of dye quenching followed the stimulus in the presence of external Ca^{2+} (Fig. 6A, inset). Equivalent results were obtained in each of six separate experiments, including four experiments with and without external Ca^{2+}. On one occasion f_{360} was seen to decay even before the end of the voltage step in the presence of external Ca^{2+}. In every case, the quenching during the first 30 s following voltage steps was accelerated in the presence of external Ca^{2+} by comparison with measurements in the absence of external Ca^{2+} (mean acceleration ± SE: $+Ca^{2+}$, 6.2 ± 0.5-fold; $-Ca^{2+}$, 0.9 ± 0.1-fold).

We interpret this behavior and the increase in fluorescence during the voltage steps to reflect the characteristics of the two divalent flux events. In the presence of external Ca^{2+}, the voltage stimulus evokes a Ca^{2+} influx and, with the Mn^{2+} electrochemical gradient directed out of the cell in the absence of external Mn^{2+}, simultaneously a Mn^{2+} efflux across the plasma membrane, which leads to an increase in Fura-2 fluorescence. The entry of Ca^{2+} then triggers Mn^{2+} release from intracellular stores and a consequent quenching of the fluorescence. That quenching is potentiated beyond the period of the voltage step implies that Mn^{2+} release continues after the voltage step and is wholly consistent with the continued rise in $[Ca^{2+}]_i$ and prolonged high $[Ca^{2+}]_i$ recorded even after voltage steps (compare Figs. 2 and 3; also see Grabov and Blatt, 1998). By contrast, in the absence of external Ca^{2+} no intracellular release is evoked and only the initial increase in fluorescence associated with Mn^{2+} efflux during the voltage step is observed.

We also tested the effects of neomycin sulfate and heparin (Fig. 6, C and D), antagonists of inositol-1,4,5-trisphosphate-mediated Ca^{2+} release, and ryanodine (Fig.

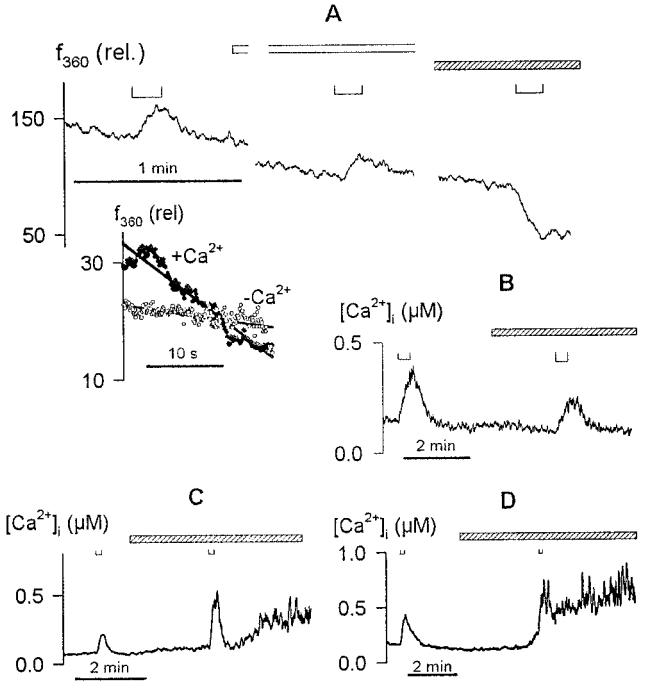

Figure 6. Evoked $[Ca^{2+}]_i$ rise is facilitated by Ca^{2+} release from intracellular stores. A, Fura-2 fluorescence quenching recorded on f_{360}. Data are from one guard cell recorded after intracellular loading with Mn^{2+} in 20 mM K^+-Mes, pH 6.1, and 2 mM $MnCl_2$. Voltage steps of 20 s to −200 mV (⊔, above) applied with the cell bathed in 20 mM K^+-Mes, pH 6.1, plus 2 mM $CaCl_2$, then in the same buffer without $CaCl_2$ (open bar), and finally with 2 mM $MnCl_2$ (striped bar). Inset, f_{360} during the first 20 s after voltage steps without (○) and with (●) Ca^{2+} outside after normalizing to the fluorescence signal at the start of each voltage step. Note the rapid decay in f_{360} after voltage stimulus in the presence of external Ca^{2+}. B to D, $[Ca^{2+}]_i$ rise was suppressed by 10 μM ryanodine (B) and augmented by 100 μM heparin (C) and 1 mM neomycin sulfate (D). Data are from three guard cells in 5 mM Ca^{2+}-Mes, pH 6.1, with 10 mM KCl. Membrane voltages were clamped to −50 mV in each case. Voltage steps to −200 mV (B) and −180 mV (C and D) are indicated above (⊔). Times of treatments with ryanodine, heparin, and neomycin sulfate are indicated by the open bars in each case. Note the prolonged secondary rise in $[Ca^{2+}]_i$ in the presence of heparin and neomycin sulfate.

6B), which blocks cADPR (ryanodine-receptor)-activated Ca^{2+} release channels (Ehrlich et al., 1994; Clapham, 1995). Of these antagonists, we found that only ryanodine antagonized the $[Ca^{2+}]_i$ response evoked by the voltage steps (Fig. 6B). In the presence of 10 μM ryanodine $[Ca^{2+}]_i$ transients recorded on negative voltage steps were reduced to 46% ± 8% (n = 5) of the control before treatments. Ryanodine also affected the rate of the $[Ca^{2+}]_i$ rise in parallel with the reduction in $[Ca^{2+}]_i$ peak amplitude (Fig. 6B). By contrast, evoked $[Ca^{2+}]_i$ transients were 1.3- to 2.5-fold greater than those recorded before treatments in the presence of 1 mM neomycin sulfate and 100 μM heparin (M_r 3000; Fig. 6, C and D), concentrations consistent with previous studies of guard cells and pollen (Armstrong and Blatt, 1995; Franklin-Tong et al., 1996). Furthermore, in the presence of these compounds the $[Ca^{2+}]_i$ transients in every case failed to recover fully and were followed by prolonged secondary increases in $[Ca^{2+}]_i$. Because neomycin sulfate and heparin can interact with ryanodine-sensitive Ca^{2+} channels (Ehrlich et al., 1994; Wang et al., 1996), these results implicate a homologous pathway for $[Ca^{2+}]_i$ release in facilitating these $[Ca^{2+}]_i$ transients.

DISCUSSION

Our demonstration of K^+ channel control by $[Ca^{2+}]_i$ establishes the $[Ca^{2+}]_i$ signal as a pivotal intermediate in feedback coupling between membrane voltage and the K^+ channels. Previous studies (Grabov and Blatt, 1998) showed that prolonged membrane hyperpolarization within the normal physiological voltage range led to a rise in $[Ca^{2+}]_i$ that was coupled to Ca^{2+} influx across the plasma membrane. The results summarized above show that, in vivo, this elevation of $[Ca^{2+}]_i$ leads to an inactivation of $I_{K,in}$ (Figs. 1–3). Remarkably, the action of $[Ca^{2+}]_i$ on the K^+ channels was realized at free concentrations only just above normal resting values (apparent K_i, 329 ± 31 nM). Furthermore, the $[Ca^{2+}]_i$ sensitivity of the current indicated a concerted action of at least four Ca^{2+} ions, leading to K^+ channel inactivation (Fig. 4). Such exquisite sensitivity to $[Ca^{2+}]_i$ has the effect of a very high gain and, hence, a narrow dynamic range for control of $I_{K,in}$. In other words, relatively small changes in $[Ca^{2+}]_i$ are able to act as a regulatory "on/off switch," transferring the K^+ channels between active and inactive states.

To our knowledge such cooperativity has not previously been documented in vivo in plant cells. Previous studies broadly defined only the limits of $[Ca^{2+}]_i$ action on $I_{K,in}$ in guard cells between 100 nM and 1 μM $[Ca^{2+}]_i$ (Schroeder and Hagiwara, 1989; Lemtiri-Chlieh and MacRobbie, 1994; Grabov and Blatt, 1997). Nonetheless, a similar degree of $[Ca^{2+}]_i$ sensitivity may be characteristic of the KCO1 K^+ channel recently cloned from Arabidopsis (Czempinski et al., 1997). It is interesting, too, that a 4-fold cooperativity is known in Ca^{2+}-signaling processes in animals (Clapham, 1995; Berridge, 1996; Cheng et al., 1996; Dolphin, 1996), including cGMP cyclase activation in vertebrate rods (Stryer and Koch, 1988). This situation, however, contrasts with pH_i control of $I_{K,in}$ that is graded over a broad range of $[H^+]_i$ and appears to depend on the binding of only one H^+ ion per channel (Grabov and Blatt, 1997).

In light of earlier studies of $[Ca^{2+}]_i$ action on $I_{K,in}$, it is worth noting the difficulties of quantifying the effects of $[Ca^{2+}]_i$ in vivo and of Ca^{2+} buffering, especially in patch-electrode experiments. In general, whole-cell patch recording results in a rapid exchange of the cytosol with the solution in the patch electrode and leads to the loss of cytosolic regulatory factors and Ca^{2+} buffering (Pusch and Neher, 1988) that may be replaced in part by Ca^{2+} buffers included in the patch pipette. Kelly et al. (1995) reported that $[Ca^{2+}]_i$ elevation suppresses $I_{K,in}$ when buffered with 1,2-bis(*o*-aminophenoxy)ethane-*N*,*N*,*N*′,*N*′-tetraacetic acid (BAPTA) but not with EGTA. They ascribed the difference to buffer efficacy, the slower kinetics of Ca^{2+}-EGTA binding, and H^+ competition with Ca^{2+} for binding to EGTA. However, because their measurements were carried out

under steady-state $[Ca^{2+}]_i$ and with pH_i held constant, the discrepancy in Ca^{2+} buffer actions remains difficult to explain. In contrast, our use of intracellular microelectrodes has the advantage that measurements are made without inclusion of Ca^{2+} buffers and with a minimum of disturbance to the cell and cytosol, because diffusional exchange with intracellular microelectrodes is restricted by the bulk access resistance of the microelectrode tip and shank (Purves, 1981).

In fact, the consequences of voltage-evoked $[Ca^{2+}]_i$ changes for the current through the K^+ channels are likely to be appreciable, as the microelectrode recordings indicate. Guard cells commonly show two states of membrane voltage that may often be separated by 100 mV or more (Thiel et al., 1992; Gradmann et al., 1993), and spontaneous membrane hyperpolarization can increase $[Ca^{2+}]_i$ from approximately 100 to 200 nM to steady-state values near 500 nM (Grabov and Blatt, 1998). Under these conditions, the positive effect of membrane hyperpolarization in activating $I_{K,in}$ will be largely overshadowed with inactivation of the current as the steady-state $[Ca^{2+}]_i$ becomes elevated. In numerical terms, hyperpolarization from −140 mV to voltages near and negative of −200 mV may still limit steady-state $I_{K,in}$ to values of approximately 10 μA cm^{-2} in the face of the $[Ca^{2+}]_i$ rise, despite the increase in electrochemical driving force and the effect of voltage otherwise on the open-channel probability (Figs. 3 and 4; see also Grabov and Blatt, 1997).

How is this rise in $[Ca^{2+}]_i$ achieved? Although the increase in $[Ca^{2+}]_i$ is triggered by Ca^{2+} influx across the plasma membrane and at voltages essentially parallel to those effective in activating $I_{K,in}$ (Grabov and Blatt, 1998), present evidence argues against Ca^{2+} entry through the K^+ channels themselves (Fairley-Grenot and Assmann, 1992). We found that the Ca^{2+} channel antagonist Gd^{3+} blocked the voltage-evoked rise in $[Ca^{2+}]_i$, and yet the same experiments showed that the antagonist actually promoted current through the K^+ channels (Fig. 5). The specificity of Gd^{3+} for Ca^{2+} channels is known to be relatively poor (Alexandre and Lassalles, 1991; Zou et al., 1991). However, the $[Ca^{2+}]_i$ rise was also sensitive to calcicludine (Fig. 5), a peptide toxin that shows high specificity for L-type Ca^{2+} channels (Schweitz et al., 1994). In contrast, voltage-evoked $[Ca^{2+}]_i$ increases were unaffected by another venom toxin, ω-conotoxin, that blocks N-type Ca^{2+} channels (Leveque et al., 1994). In complementary experiments we observed that the $[Ca^{2+}]_i$ rise was independent of extracellular K^+ (Grabov and Blatt, 1998) and was unaffected by block of the K^+ current with Cs^+. Were a significant flux of Ca^{2+} to pass through the K^+ channels, both competition with K^+ and Cs^+ block might have been expected to reduce the $[Ca^{2+}]_i$ rise. So, the simplest interpretation is that Ca^{2+} entry across the plasma membrane occurs through hyperpolarization-activated Ca^{2+} channels. In fact, a sensitivity to membrane hyperpolarization may be a common feature of many Ca^{2+} channels in the plant plasma membrane, although it remains to be seen whether hyperpolarization-activated Ca^{2+} channels of higher plants are found predominantly in specialized cells, such as guard cells. Hyperpolarization-activated Ca^{2+} channels have also been reported in tomato plasma membrane (Gelli and Blumwald, 1997), and there are indications of similar Ca^{2+} channels in *Mimosa pudica* (Stoeckel and Takeda, 1995).

Elevation of $[Ca^{2+}]_i$ by membrane hyperpolarization also appears to depend on Ca^{2+} release from intracellular stores. We observed an accelerated quenching of Fura-2 fluorescence by intracellular (sequestered) Mn^{2+} following voltage steps when guard cells were preloaded with the divalent cation, and the results of studies with Ca^{2+} release antagonists lead to a similar conclusion (Fig. 6). Block of the voltage-evoked $[Ca^{2+}]_i$ rise by ryanodine, and its stimulation by heparin and neomycin sulfate, suggests a parallel to ryanodine-receptor Ca^{2+} channels that mediate Ca^{2+} release in neuromuscular tissues (Ehrlich et al., 1994; Clapham, 1995). The fact that ryanodine block was incomplete may reflect the relatively short exposures that could be achieved within the time frame of these experiments, or it may indicate a significant contribution of external Ca^{2+} influx to the rise in $[Ca^{2+}]_i$. However, we cannot rule out additional contributions to $[Ca^{2+}]_i$ release via inositol-1,4,5-trisphosphate-sensitive or other unrelated pathways (Cheek et al., 1994; Jouaville et al., 1995). We also noted a dependence of voltage-evoked $[Ca^{2+}]_i$ increases on the resting $[Ca^{2+}]_i$ level before stimulation (Fig. 2D). A similar sensitivity to $[Ca^{2+}]_i$ is common to many Ca^{2+}-release events in animals that show a bell-shaped curve characteristic of potentiation by $[Ca^{2+}]_i$ (Callamaras and Parker, 1994; Bezprozvanny and Ehrlich, 1995; Cheng et al., 1996; Thorn et al., 1996).

These parallels to Ca^{2+} release events in animals do raise questions about the nature of the guard cell Ca^{2+}-release pathway and the location of the Ca^{2+} stores. It is possible, for example, that $[Ca^{2+}]_i$ changes are mediated by spatially distinct Ca^{2+} stores with different characteristics for Ca^{2+} release (Bootman and Berridge, 1996; Plieth et al., 1998). Thus, conceivably, short-term dynamic control of $I_{K,in}$ might be more closely coupled to $[Ca^{2+}]_i$ and Ca^{2+} release events close to the plasma membrane, in contrast to the current characteristics determined under quasi-steady-state $[Ca^{2+}]_i$, as described above. In this context, we note that ryanodine affects Ca^{2+} release from plant microsomes but acts to stimulate Ca^{2+} release even at micromolar concentrations (Allen et al., 1995; Muir and Sanders, 1996), in contrast to our observations (Fig. 6B). Furthermore, despite the presumed role for vacuolar Ca^{2+} in plant cell (and guard cell) signaling (Ward and Schroeder, 1994; Allen and Sanders, 1995, 1996; Johannes and Sanders, 1995), one recent study indicated that evoked Ca^{2+} release in the alga *Chara* does not depend on vacuolar Ca^{2+} stores (Plieth et al., 1998). Therefore, it is conceivable that the $[Ca^{2+}]_i$ signal in the guard cells draws on more than one Ca^{2+}-release pathway, each with differing pharmacological characteristics and, possibly, separate Ca^{2+} stores. Such issues aside, these and our previous observations (Grabov and Blatt, 1998) implicate the coordination of Ca^{2+} influx and Ca^{2+} release from intracellular stores that parallels CICR events in animal cells (Clapham, 1995; Berridge, 1996). Again, the data also underscore at least one important difference from the animal models. The $[Ca^{2+}]_i$ rise in the guard cells was evoked at negative voltages, whereas voltage-evoked CICR

in neuromuscular tissues is normally triggered by membrane depolarization that activates Ca^{2+} influx through pharmacologically distinct, L-type Ca^{2+} channels (Schweitz et al., 1994; Chavis et al., 1996).

What are the physiological roles for coupling $I_{K,in}$ to membrane voltage through $[Ca^{2+}]_i$ and for the high gain inherent in $I_{K,in}$ inactivation by $[Ca^{2+}]_i$? One clue may lie in voltage oscillations that have been observed in guard cells (Thiel et al., 1992; Gradmann et al., 1993). These oscillations occur spontaneously, they are potentiated by ABA and auxin that effect stomatal movements (Thiel et al., 1992; Blatt and Thiel, 1994), and they may be aperiodic or exhibit periodicities of 10 to 20 s (Gradmann et al., 1993) to many minutes (Thiel et al., 1992; Blatt and Thiel, 1994). These events arise through fluctuations in the activities of the K^+ and anion channels (Blatt and Thiel, 1994) similar to those of the action potentials in Characean algae (Beilby, 1986). The effect is to drive the membrane between the hyperpolarized state, characterized by K^+ uptake via $I_{K,in}$ and balanced by H^+ efflux through the H^+-ATPase, and the depolarized state, in which efflux of K^+ and anions dominate. Significantly, $[Ca^{2+}]_i$ elevation leads to inhibition of the H^+-ATPase (Kinoshita et al., 1995) and $I_{K,in}$ (Figs. 3 and 4), as well as activation of anion channels (Hedrich et al., 1990; Schroeder and Keller, 1992). Inhibition of the H^+-ATPase shows an apparent K_d of approximately 300 nM, similar to what we found for $I_{K,in}$ (Fig. 4). We (Grabov and Blatt, 1998) previously demonstrated the coupling of $[Ca^{2+}]_i$ to membrane voltage and suggest now that its function may be to provide the necessary feedback to entrain K^+ and anion channels as a response "cassette" for osmotic balance, switching the membrane between states for net uptake and net loss of these solutes (Gradmann et al., 1993).

Coupling to membrane voltage may also serve to "condition" $[Ca^{2+}]_i$ signals that are triggered in response to hormones and other stimuli (Grabov and Blatt, 1998). Downstream of the initial stimulus, effective control of the ion channels and solute flux requires that second-messenger "signatures" correctly reflect the needs for change in solute flux dictated by the prior transport status of the cell. Thus, a second function for voltage coupling may lie in adapting the $[Ca^{2+}]_i$ signal output on stimulation to the prevailing requirements for solute flux. In the simplest sense, if the purpose of a rise in $[Ca^{2+}]_i$, for example, in response to ABA (Blatt and Grabov, 1997; Thiel and Wolf, 1997), is to trigger membrane depolarization when the voltage is situated well negative of the K^+ equilibrium voltage E_K, the same $[Ca^{2+}]_i$ rise will be superfluous should the membrane already be situated at a voltage positive of E_K and, hence, biased for solute loss. In fact, ABA does not evoke significant $[Ca^{2+}]_i$ increases when the membrane voltage is clamped near -50 mV but only when the voltage is situated near or negative of -100 mV (Grabov and Blatt, 1998). These ideas lend a further dimension to concepts of frequency encoding (Campbell et al., 1996; Knight et al., 1996) and to our understanding of $[Ca^{2+}]_i$ oscillations in plants (McAinsh et al., 1995; Webb et al., 1996), and they raise issues relating to the spatiokinetic mechanics that couple membrane voltage, Ca^{2+} influx, and Ca^{2+} release at the subcellular level.

In conclusion, we find that inactivation of $I_{K,in}$ by $[Ca^{2+}]_i$ appears to depend on the cooperative action of four Ca^{2+} ions, conferring on the K^+ channels a very steep dependence on $[Ca^{2+}]_i$ in the free-concentration range just above normal resting values. Such $[Ca^{2+}]_i$ increases in broad bean guard cells can be evoked on membrane hyperpolarization within the normal physiological voltage range and thus couple $I_{K,in}$ activity to membrane voltage in a negative-feedback control loop. We also find that voltage-evoked $[Ca^{2+}]_i$ increases depend on intracellular Ca^{2+} release and on Ca^{2+} influx, the latter occurring via a pathway that is pharmacologically distinct from $I_{K,in}$. These observations implicate a process of CICR with characteristics that differ markedly from the conventional neuromuscular models and suggest a function in coordinate control of K^+, H^+, and anion transport for osmotic balance.

Received June 11, 1998; accepted September 24, 1998.

LITERATURE CITED

Alexandre J, Lassalles JP (1991) Hydrostatic and osmotic pressure activated channel in plant vacuole. Biophys J **60:** 1326–1336

Allen GJ, Muir SR, Sanders D (1995) Release of Ca^{2+} from individual plant vacuoles by both insp(3) and cyclic ADP-ribose. Science **268:** 735–737

Allen GJ, Sanders D (1995) Calcineurin, a type 2B protein phosphatase, modulates the Ca^{2+}-permeable slow vacuolar ion channel of stomatal guard cells. Plant Cell **7:** 1473–1483

Allen GJ, Sanders D (1996) Control of ionic currents in guard cell vacuoles by cytosolic and luminal calcium. Plant J **10:** 1055–1069

Armstrong F, Blatt MR (1995) Evidence for K^+ channel control in *Vicia* guard cells coupled by G-proteins to a 7TMS receptor. Plant J **8:** 187–198

Beilby MJ (1986) Potassium channels and different states of the *Chara* plasmalemma. J Membr Biol **89:** 241–249

Berridge MJ (1996) Microdomains and elemental events in calcium signaling. Cell Calcium **20:** 95–96

Bezprozvanny I, Ehrlich BE (1995) The inositol 1,4,5-trisphosphate (insp3) receptor. J Membr Biol **145:** 205–216

Blatt MR, Armstrong F (1993) K^+ channels of stomatal guard cells: abscisic acid-evoked control of the outward rectifier mediated by cytoplasmic pH. Planta **191:** 330–341

Blatt MR, Grabov A (1997) Signalling gates in abscisic acid-mediated control of guard cell ion channels. Physiol Plant **100:** 481–490

Blatt MR, Thiel G (1994) K^+ channels of stomatal guard cells: bimodal control of the K^+ inward-rectifier evoked by auxin. Plant J **5:** 55–68

Bootman MD, Berridge MJ (1996) Subcellular Ca^{2+} signals underlying waves and graded responses in HeLa cells. Curr Biol **6:** 855–865

Callamaras N, Parker I (1994) Inositol 1,4,5-trisphosphate receptors in *Xenopus laevis* oocytes—localization and modulation by Ca^{2+}. Cell Calcium **15:** 66–78

Campbell AK, Trewavas AJ, Knight MR (1996) Calcium imaging shows differential sensitivity to cooling and communication in luminous transgenic plants. Cell Calcium **19:** 211–218

Chavis P, Fagni L, Lansman JB, Bockaert J (1996) Functional coupling between ryanodine receptors and L-type calcium channels in neurons. Nature **382:** 719–722

Cheek TR, Berridge MJ, Moreton RB, Stauderman KA, Murawsky MM, Bootman MD (1994) Quantal Ca^{2+} mobilization by

ryanodine receptors is due to all-or-none release from functionally discrete intracellular stores. Biochem J **301:** 879–883

Cheng H, Lederer MR, Xiao RP, Gomez AM, Zhou YY, Ziman B, Spurgeon H, Lakatta EG, Lederer WJ (1996) Excitation-contraction coupling in heart—new insights from Ca^{2+} sparks. Cell Calcium **20:** 129–140

Clapham DE (1995) Calcium signaling. Cell **80:** 259–268

Czempinski K, Zimmermann S, Ehrhardt T, MullerRober B (1997) New structure and function in plant K^+ channels: KCO1, an outward rectifier with a steep Ca^{2+} dependency. EMBO J **16:** 2565–2575

Dolphin AC (1996) Facilitation of Ca^{2+} current in excitable cells. Trends Neurosci **19:** 35–43

Ehrlich BE, Kaftan E, Bezprozvannaya S, Bezprozvanny I (1994) The pharmacology of intracellular Ca^{2+}-release channels. Trends Pharmacol Sci **15:** 145–149

Fairley-Grenot KA, Assmann SM (1992) Permeation of Ca^{2+} through K^+ channels in the plasma membrane of *Vicia faba* guard cells. J Membr Biol **128:** 103–113

Fasolato C, Hoth M, Matthews G, Penner R (1993) Ca^{2+} and Mn^{2+} influx through receptor-mediated activation of nonspecific cation channels in mast cells. Proc Natl Acad Sci USA **90:** 3068–3072

Franklintong VE, Drobak BK, Allan AC, Watkins PAC, Trewavas AJ (1996) Growth of pollen tubes of *Papaver rhoeas* is regulated by a slow-moving calcium wave propagated by inositol 1,4,5-trisphosphate. Plant Cell **8:** 1305–1321

Gelli A, Blumwald E (1997) Hyperpolarization-activated Ca^{2+}-permeable channels in the plasma membrane of tomato cells. J Membr Biol **155:** 35–45

Grabov A, Blatt MR (1997) Parallel control of the inward-rectifier K^+ channel by cytosolic-free Ca^{2+} and pH in *Vicia* guard cells. Planta **201:** 84–95

Grabov A, Blatt MR (1998) Membrane voltage initiates Ca^{2+} waves and potentiates Ca^{2+} increases with abscisic acid in stomatal guard cells. Proc Natl Acad Sci USA **95:** 4778–4783

Gradmann D, Blatt MR, Thiel G (1993) Electrocoupling of ion transporters in plants. J Membr Biol **136:** 327–332

Hammondkosack KE, Jones JDG (1997) Plant disease resistance genes. Annu Rev Plant Physiol Plant Mol Biol **48:** 575–607

Hedrich R, Busch H, Raschke K (1990) Ca^{2+} and nucleotide dependent regulation of voltage dependent anion channels in the plasma membrane of guard cells. EMBO J **9:** 3889–3892

Hill AV (1910) The possible effects of the aggregation of the molecules of hemoglobin on its dissociation curves. J Physiol **40:** 4–7

Hosoi S, Iino M, Shimazaki K (1988) Outward-rectifying K^+ channels in stomatal guard cell protoplasts. Plant Cell Physiol **29:** 907–911

Johannes E, Sanders D (1995) The voltage-gated Ca^{2+} release channel in the vacuolar membrane of sugar beet resides in 2 activity states. FEBS Lett **365:** 1–6

Jouaville LS, Ichas F, Holmuhamedov EL, Camacho P, Lechleiter JD (1995) Synchronization of calcium waves by mitochondrial substrates in *Xenopus laevis* oocytes. Nature **377:** 438–441

Kelly WB, Esser JE, Schroeder JI (1995) Effects of cytosolic calcium and limited, possible dual, effects of G-protein modulators on guard cell inward potassium channels. Plant J **8:** 479–489

Kinoshita T, Nishimura M, Shimazaki KI (1995) Cytosolic concentration of Ca^{2+} regulates the plasma membrane H^+-ATPase in guard cells of fava bean. Plant Cell **7:** 1333–1342

Klusener B, Boheim G, Liss H, Engelberth J, Weiler EW (1995) Gadolinium-sensitive, voltage-dependent calcium release channels in the endoplasmic reticulum of a higher-plant mechanoreceptor organ. EMBO J **14:** 2708–2714

Knight H, Trewavas AJ, Knight MR (1996) Cold calcium signaling in *Arabidopsis* involves 2 cellular pools and a change in calcium signature after acclimation. Plant Cell **8:** 489–503

Lemtiri-Chlieh F, MacRobbie EAC (1994) Role of calcium in the modulation of *Vicia* guard cell potassium channels by abscisic acid: a patch-clamp study. J Membr Biol **137:** 99–107

Leveque C, Elfar O, Martinmoutot N, Sato K, Kato R, Takahashi M, Seagar MJ (1994) Purification of the N-type calcium-channel associated with syntaxin and synaptotagmin—a complex implicated in synaptic vesicle exocytosis. J Biol Chem **269:** 6306–6312

Low PS, Merida JR (1996) The oxidative burst in plant defense—function and signal transduction. Physiol Plant **96:** 533–542

Marquardt D (1963) An algorithm for least-squares estimation of nonlinear parameters. J Soc Ind Appl Math **11:** 431–441

McAinsh MR, Brownlee C, Hetherington AM (1997) Calcium ions as second messengers in guard cell signal transduction. Physiol Plant **100:** 16–29

McAinsh MR, Webb AAR, Taylor JE, Hetherington AM (1995) Stimulus-induced oscillations in guard cell cytosolic-free calcium. Plant Cell **7:** 1207–1219

Mori Y, Friedrich T, Kim M-S, Mikami A, Nakai J, Ruth P, Bosse E, Hofmann F, Flockerzi V, Furuichi T, and others (1991) Primary structure and functional expression from complementary DNA of a brain calcium channel. Nature **350:** 398–402

Muir SR, Sanders D (1996) Pharmacology of Ca^{2+} release from red beet microsomes suggests the presence of ryanodine receptor homologs in higher-plants. FEBS Lett **395:** 39–42

Pineros M, Tester M (1995) Characterization of a voltage-dependent Ca^{2+}-selective channel from wheat roots. Planta **195:** 478–488

Plieth C, Sattelmacher B, Hansen UP, Thiel G (1998) The action potential in *Chara*: Ca^{2+} release from internal stores visualized by Mn^{2+}-induced quenching of fura-dextran. Plant J **13:** 167–175

Purves JD (1981) Microelectrode Methods for Intracellular Recording and Ionophoresis, Vol 1. Academic Press, London, pp 1–146

Pusch M, Neher E (1988) Rates of diffusional exchange between small cells and a measuring patch pipette. Pflugers Archiv Eur J Physiol **411:** 204–214

Russell AJ, Knight MR, Cove DJ, Knight CD, Trewavas AJ, Wang TL (1996) The moss, *Physcomitrella patens*, transformed with apoaequorin cDNA responds to cold shock, mechanical perturbation and pH with transient increases in cytoplasmic calcium. Transgenic Res **5:** 167–170

Schofield GG, Mason MJ (1996) A Ca^{2+} current activated by release of intracellular Ca^{2+} stores in rat basophilic leukemia cells (RBL-1). J Membr Biol **153:** 217–231

Schroeder JI (1988) K^+ transport properties of K^+ channels in the plasma membrane of *Vicia faba* guard cells. J Gen Physiol **92:** 667–683

Schroeder JI, Hagiwara S (1989) Cytosolic calcium regulates ion channels in the plasma membrane of *Vicia faba* guard cells. Nature **338:** 427–430

Schroeder JI, Keller BU (1992) Two types of anion channel currents in guard cells with distinct voltage regulation. Proc Natl Acad Sci USA **89:** 5025–5029

Schweitz H, Heurteaux C, Bois P, Moinier D, Romey G, Lazdunski M (1994) Calcicludine, a venom peptide of the Kunitz-type protease inhibitor family, is a potent blocker of high-threshold Ca^{2+} channels with a high-affinity for L-type channels in cerebellar granule neurons. Proc Natl Acad Sci USA **91:** 878–882

Sedbrook JC, Kronebusch PJ, Borisy CG, Trewavas AJ, Masson PH (1996) Transgenic aequorin reveals organ-specific cytosolic Ca^{2+} responses to anoxia in *Arabidopsis thaliana* seedlings. Plant Physiol **111:** 243–257

Stoeckel H, Takeda K (1995) Calcium-sensitivity of the plasmalemmal delayed rectifier potassium current suggests that calcium influx in pulvinar protoplasts from *Mimosa pudica* l can be revealed by hyperpolarization. J Membr Biol **146:** 201–209

Striggow F, Ehrlich BE (1996) The inositol 1,4,5-trisphosphate receptor of cerebellum—Mn^{2+} permeability and regulation by cytosolic Mn^{2+}. J Gen Physiol **108:** 115–124

Stryer L, Koch K-W (1988) Highly cooperative feedback control of retinal rod guanylate cyclase by calcium ions. Nature **334:** 64–66

Thiel G, MacRobbie EAC, Blatt MR (1992) Membrane transport in stomatal guard cells: the importance of voltage control. J Membr Biol **126:** 1–18

Thiel G, Wolf AH (1997) Operation of K^+ channels in stomatal movement. Trends Plant Sci **2:** 339–345

Thorn P, Moreton R, Berridge M (1996) Multiple, coordinated Ca^{2+}-release events underlie the inositol trisphosphate-induced local Ca^{2+} spikes in mouse pancreatic acinar cells. EMBO J **15:** 999–1003

Wang JP, Needleman DH, Seryshev AB, Aghdasi B, Slavik KJ, Liu SQ, Pedersen SE, Hamilton SL (1996) Interaction between ryanodine and neomycin binding sites on Ca^{2+} release channel from skeletal muscle sarcoplasmic reticulum. J Biol Chem **271:** 8387–8393

Ward JM, Schroeder JI (1994) Calcium-activated K^+ channels and calcium-induced calcium release by slow vacuolar ion channels in guard-cell vacuoles implicated in the control of stomatal closure. Plant Cell **6:** 669–683

Webb AAR, McAinsh MR, Mansfield TA, Hetherington AM (1996) Carbon dioxide induces increases in guard cell cytosolic free calcium. Plant J **9:** 297–304

Zou XL, Stumpf MA, Hoch HC, Kung C (1991) A mechanosensitive channel in whole cells and in membrane patches of the fungus *Uromyces*. Science **253:** 1415–1417